online data

Original Paper

Ser^{262} determines the chloride-dependent colour tuning of a new halorhodopsin from *Haloquadratum walsbyi*

Hsu-Yuan FU*[1], Yung-Ning CHANG*[1], Ming-Jin JHENG* and Chii-Shen YANG*†[2]

*Department of Biochemical Science and Technology, College of Life Science, National Taiwan University, 1 Roosevelt Road, Taipei 10617, Taiwan, and †Institute of Biotechnology, College of Bio-Resources and Agriculture, National Taiwan University, 1 Roosevelt Road, Taipei 10617, Taiwan

Synopsis

Light is an important environmental signal for all organisms on earth because it is essential for physiological signalling and the regulation of most biological systems. Halophiles found in salt-saturated ponds encode various archaeal rhodopsins and thereby harvest various wavelengths of light either for ion transportation or as sensory mediators. HR (halorhodopsin), one of the microbial rhodopsins, senses yellow light and transports chloride or other halides into the cytoplasm to maintain the osmotic balance during cell growth, and it exists almost ubiquitously in all known halobacteria. To date, only two HRs, isolated from *Hs*HR (*Halobacterium salinarum* HR) and *Np*HR (*Natronomonas pharaonis* HR), have been characterized. In the present study, two new HRs, *Hm*HR (*Haloarcula marismortui* HR) and *Hw*HR (*Haloquadratum walsbyi* HR), were functionally overexpressed in *Escherichia coli*, and the maximum absorbance (λ_{max}) of the purified proteins, the light-driven chloride uptake and the chloride-binding affinity were measured. The results showed them to have similar properties to two HRs reported previously. However, the λ_{max} of *Hw*HR is extremely consistent in a wide range of salt/chloride concentrations, which had not been observed previously. A structural-based sequence alignment identified a single serine residue at 262 in *Hw*HR, which is typically a conserved alanine in all other known HRs. A Ser^{262} to alanine replacement in *Hw*HR eliminated the chloride-independent colour tuning, whereas an Ala^{246} to serine mutagenesis in *Hs*HR transformed it to have chloride-independent colour tuning similar to that of *Hw*HR. Thus Ser^{262} is a key residue for the mechanism of chloride-dependent colour tuning in *Hw*HR.

Key words: chloride affinity, halorhodopsin, light-driven chloride pump, photocycle, spectral tuning, site-directed evolution

INTRODUCTION

Solar light is a crucial environmental signal for most life forms, as it is intricately involved in energy harvesting and many physiological signals, including circadian rhythm and photo-taxic responses [1]. Featuring biological systems with light-driven systems, halophiles are known to exist widely in salt-saturated ponds. They encode four types of archaeal rhodopsins that respond to different wavelengths of light either by transporting ions, as observed in BR (bacteriorhodopsin) and HR (halorhodopsin) [2–4], or by serving as illumination sensors that trigger different phototaxic responses typified by the SRs (sensory rhodopsins) I and II found in *Halobacterium salinarium* [5–7].

All four types of microbial rhodopsins are not simultaneously encoded in the genome of a single species as they are in *H. salinarum* [1]. Only one HR and one SRII were found to exist in *Natronomonas pharaonis* [8], whereas one BR, one HR and one MR (middle rhodopsin) with ambiguous function were identified in *H. walsbyi* without any SR [9,10]. *H. marismortui*, by contrast, encodes six rhodopsins, including two BRs, one HR, SRI, SRII and SRM, which is the greatest number of microbial rhodopsins found in a single archaeon [11,12].

HR, however, is the most prevalent microbial rhodopsin in archaea. More than a dozen HRs have been either confirmed by protein studies or proposed in various genomic projects (Supplementary Table S1 at http://www.bioscirep.org/bsr/032/bsr0320501add.htm). The first HR was identified in *Hs*HR (*H. salinarum* HR) and the second one was later found in *Np*HR (*N. pharaonis* HR). Previous studies have described HRs as light-driven inward anion/chloride translocators and have suggested that they facilitate BR-assisted energy production [13] and preserve the cytoplasmic osmolality equilibrium [4]. HRs therefore assist cells in producing energy and maintaining their cellular environments. It is reasonable to expect to find HRs in almost any microbe residing in a hypersaline habitat, as HRs play such an essential role for cell survival in crystallizer conditions.

Various biological and biophysical properties of *Hs*HR and *Np*HR have been reported [14–16]; both HRs have been shown to absorb light maximally at approximately 575 nm, and the light-activated HRs initialize inward transport of chloride and other halides (Br$^-$, I$^-$) [17]. The molecular mechanism for this light-driven chloride transport has been investigated in several crystallography studies for both *Hs*HR and *Np*HR [18,19]. Further studies have shown their similarity in chloride-binding affinities [20,21], pK_a [20,22] and ms-ranged photocycle kinetics [23], as well as shifts in their λ_{max} (maximum absorbance wavelengths) under low-chloride or low-salt concentrations. The environment-dependent λ_{max} shift is one of the main reasons that an engineered HR such as *Np*HR 3.0 [24], a mutant based on *Np*HR that was designed to serve as a nerve de-activation signal, was developed for optogenetic technology.

The HR gene proposed in the *H. walsbyi* genome [9] is intriguing because *H. walsbyi* cells are one of the most widely distributed halobacteria, globally present from shallow ocean coastal areas to crystallized ponds [25], with a variety of chloride concentrations. All HRs from other species were shown to be sensitive to chloride concentrations [20,21]. The ability of this newly proposed *Hw*HR (*H. walsbyi* HR) to survive in environments with great variation in salinity or osmolality is investigated in the present study.

The *Hw*HR, together with *Hm*HR (*Haloarcula marismortui* HR), was first overexpressed and then purified for *in vitro* characterization. Both *Hm*HR and *Hw*HR were found to share most of the conserved functions and properties that have been observed for other known HRs; however, *Hw*HR showed unique salt-independent changes in λ_{max}, a feature not observed in any of the other HR proteins characterized to date. A single residue substitution, which was chosen via structure-based sequence alignment, eliminated such chloride-independent spectral tuning.

MATERIALS AND METHODS

Bacterial strains and plasmids

Escherichia coli DH5α cells were used for cloning and *E. coli* C43(DE3) cells were used for protein expression.

The genes of *Hm*HR [12] and *Hs*HR [26] were cloned from genomic DNA, and HwHR [9] was synthesized by Genomics with the addition of a NcoI restriction enzyme cutting site before the start codon and a XhoI restriction enzyme cutting site after the stop codon. The DNA fragment was treated with restriction enzymes and ligated into a NcoI–XhoI-treated pET-21d vector. As described previously [27], the expressed N- and C-terminal peptide sequences are as follows: *Hm*HR: ^{1}MTAAST . . . . . . .TPADD^{276}KLAAALEHHHHHH and *Hw*HR: ^{1}MAQHLY . . . . . . .AVADD^{292}LEHHHHHH. The site-directed mutagenesis was performed according to the instruction manual from the QuikChange^{TM} Lightning Site-Directed Mutagenesis Kit.

Protein expression and purification

A single colony of transformed *E. coli* C43(DE3) cells was inoculated in LB (Luria–Bertani) medium supplemented with 50 μg/ml of ampicillin and incubated at 37°C overnight. For large-scale protein expression, a 1:100 (v/v) dilution of overnight culture was added to a fresh LB/ampicillin medium and incubated at 37°C. When the D_{600} of the culture reached 0.4–0.6, IPTG (iso-propyl β-D-1-thiogalactopyranoside; final concentration 1 mM) and all-*trans* retinal (final concentration 5–10 μM) were added for induction. Following subsequent incubation for 4–6 h in the dark, cells were collected by centrifugation at 6750 ***g*** for 10 min at 4°C (Hitachi CR-21, R10A3). The collected cells were re-suspended in buffer A (50 mM Tris/HCl, 4 M NaCl, 14.7 mM 2-mercaptoethanol and 0.2 mM PMSF, pH 7.8) and broken by ultrasonic processing (S-3000; MISONIC). For the separation of the membrane fraction, total cell-extract centrifugation was performed at 2330 ***g*** for 30 min at 4°C (KUBOTA 5910). Then, the supernatant was centrifuged at 169 538 ***g*** for 1 h at 4°C (Beckman L-90, Ti-70). The sediment was dissolved in buffer B (buffer A supplemented with 1% DDM (n-dodecyl-β-D-maltoside) for at least 12 h at 4°C, followed by centrifugation at 32 816 ***g*** for 45 min at 4°C (Hitachi CR-21, R20A2) to separate the detergent-soluble fraction. Solubilized HRs were purified by affinity purification using the Ni-NTA (Ni^{2+}-nitrilotriacetate) method. The detergent-soluble solution containing 20 mM imidazole was incubated with Ni-NTA agarose at 4°C for 6–8 h of slow nutation. It was then transferred to a chromatography column and washed with buffer C (buffer A with 0.05% DDM and 50 mM imidazole). The target HRs were eluted with buffer D (buffer A with 0.05% DDM and 250 mM imidazole). Purified HRs were concentrated and exchanged into buffer E (50 mM Mes, 4 M NaCl and 0.05% DDM, pH 5.8) with a protein concentrator (Millipore, Amicon, cut-off size of 30 kDa).

Light-driven ion transporter assay

E. coli cells with overexpressed HR were prepared as described previously using protein overexpression and purification protocols [12,28]. Induced cells without all-*trans* retinal addition served as a control. The collected cells were washed twice using an unbuffered solution (10 mM NaCl, 10 mM MgSO$_4$ and

100 μM CaCl$_2$) and suspended with an adequate amount of fresh buffer. The suspended cells were illuminated with green laser light, and the extracellular pH change was monitored with a probe (Eutech Instruments, CyberScan pH 2100). After 100 s of illumination, the dark incubation of an additional 100 s was also recorded. The illumination followed by dark incubation procedure was repeated three times. To check for passive proton uptake, experiments using suspended cells with CCCP (carbonyl cyanide *m*-chlorophenylhydrazone; Sigma C2759; to a final concentration of 10 μM) were performed as described above. All pH changes were recorded with the CyberComm Pro program and exported as .csv files.

pK_a determination

The purified proteins were diluted with buffers at different pH values (100-fold dilution). UV/Vis absorption spectra of 12 protein samples of pHs varying from 5.8 to 10.93 were recorded. To evaluate the wavelength that indicated the maximum absorbance change, all spectra were plotted together or subtracted. In HRs, the acidic–basic absorbance at 575 nm (*Hm*HR) and 572 nm (*Hw*HR) was calculated in relative units and plotted against the pH values. The sigmoid curve generated was fit to the following equation: $\text{Abs} = \text{Abs}_{acidic} + \text{Abs}_{basic\text{-}acidic} \times (10^{pH - pK_a})$. A similar equation named DoseResp in Origin® was also used: $y = A_1 + (A_2 - A_1)/1 + 10^{(LOGx0 - x)p}$; the symbol LOGx0 was denoted as the pK_a value.

Chloride titration assay

The purified *Hw*HR was adjusted to different chloride concentrations to determine the chloride-binding affinity as described in previous studies with a slight modification [19,20]. The NaCl concentration was reduced from 4 M to 0.015 mM in a 50 mM Mes buffer, pH 5.8 (or in 50 mM Mops buffer, pH 7.0) At each chloride concentration, the UV/Vis spectrum was recorded and normalized using A_{280} as a standard. The amplitude changes of the absorbance in relative units were plotted against the chloride concentration (log10 scale), then the resulting curve was fitted to the Hill equation ($R^2 > 0.95$). The following Hill equation was adopted for analysis: $y = (V_{max} \times x^n)/(k^n + x^n)$; k denotes the dissociation constant.

Flash-laser induced photocycle measurements

Nd-YAG laser (532 nm, 6 ns pulse, 40 mJ) flash-absorbance changes were measured by employing a laboratory-constructed laser cross-beam flash spectrometer as previously described [12]. The purified proteins were dissolved in buffer E to reach 0.3 at a maximum-wavelength (λ_{max}) (A_{max}), and transient-absorbance changes were recorded at their corresponding ground-state maximum. The curves represent the loss and recovery of absorbance at the target wavelengths upon green laser ($\lambda_{ex} = 532$ nm).

RESULTS

Sequence alignment of known and proposed HR genes from *Halobacteria*

HRs are prevalent in *Halobacteria*; more than 15 strains (Supplementary Table S1) of *Halobacteria* have been completely sequenced to date, and at least nine of these were proven or predicted to have *hop* genes. A phylogenic tree (Figure 1a) and sequence alignment (Figure 1b, and Supplementary Figure S1 at http://www.bioscirep.org/bsr/032/bsr0320501add.htm) of 17 annotated HRs showed high sequence identity (55–68%) among them, and the previously reported key residues involved in chloride transportation, i.e. Arg[108]/Thr[111] and Arg[200]/Thr[203] in *Hs*HR [18], were found to be conserved in all HRs. Although the classification of HRs were not correlated with the evolution [29], *Hm*HR and *Hw*HR, which were the focus in the present study, showed higher sequence similarity with *Np*HR and *Hs*HR respectively.

Purification and spectral characterization of *Hm*HR and *Hw*HR

To examine and compare the spectral characteristics of HR proteins, we overexpressed and purified His$_6$-tagged *Hm*HR and *Hw*HR proteins using the *E. coli* C43(DE3) system according to previously described protocols [12]. This procedure yielded several mg/l of culture.

The UV/Vis spectra showed the λ_{max} of *Hm*HR to be 576 nm (Figure 2a), whereas the λ_{max} of *Hw*HR was 573 nm (Figure 2b). Compared with all well-known HRs, all of them were within approximately 3 nm of 575 nm (summarized in Supplementary Table S3 at http://www.bioscirep.org/bsr/032/bsr0320501add.htm).

Light-driven chloride transport activity measurements

Light-driven inward chloride transport measurements for *Hm*HR and *Hw*HR were performed to examine their function as illumination-dependent chloride translocators, using previously described procedures [12]. Light-dependent pH increases were recorded in both *Hm*HR (Figure 2c) and *Hw*HR (Figure 2d) samples with or without CCCP. The observed tendency of light-driven proton transport in both HRs were in fact passive processes accelerated by light-driven chloride inward transportation as explained in a previous study [27], indicating that light-driven inward chloride transport occurred. Thus both *Hm*HR and *Hw*HR proteins demonstrated light-driven inward chloride transport, confirming their conserved function as observed in two other HRs.

Flash laser-induced absorbance changes of *Hm*HR and *Hw*HR

To investigate the photocycle, the defining feature of the two HRs, time-resolved flash photolysis was measured. The data
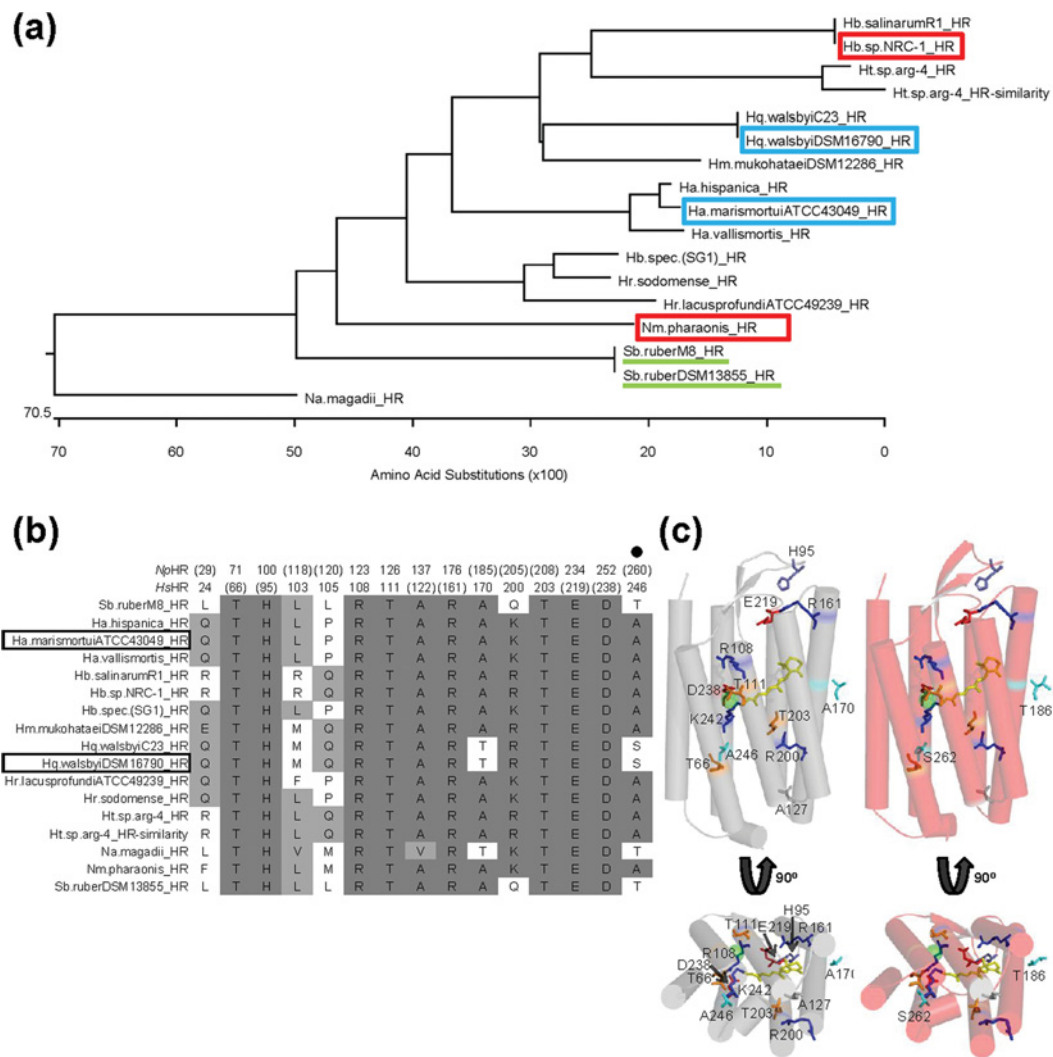
Figure 1   Bioinformatic analysis of microbial HRs and structural alignment of *Hs*HR and *Hw*HR
(**a**) Phylogenetic tree of 17 annotated microbial HRs. The green-underlined organisms are the sources of the two HRs from bacteria. The red rectangles indicate the two well-studied HRs from *Halobacterium salinarum* and *Natronobacterium pharaonis*; the blue rectangles indicate the two HRs from *Hm*HR and *Hw*HR in the present study. (**b**) Amino acid sequence alignment of critical residues involved in chloride translocation and of interest in the present study. The first two rows are numbered with the atomic resolution structures based on *Np*HR (PDB ID: 3A7K) and *Hs*HR (PDB ID: 1E12). The black rectangles indicate the two HRs in the present study. The shadowed grey scale marks the conserved residues, and the critical spectral tuner one is annotated with the black spot. (**c**) Structural information of *Hs*HR (grey, PDB ID: 1E12) and *Hw*HR (red, modelled by SWISS-MODEL). The conserved chloride transport residues (stick) are labelled with their name and number (Thr^{66}, His^{95}, Arg^{108}, Thr^{111}, Ala^{127}, Arg^{161}, Arg^{200}, Thr^{203}, Glu^{219} and Asp^{238}). The yellow stick is *all-trans* retinal; the conserved residues Thr^{111} and Asp^{238} harbour a chloride ion (green sphere) in the structures of *Hs*HR and *Hw*HR. The residues (cyan stick) indicate the mutated site of *Hw*HR in this study. The top is the periplasmic region and the bottom is the cytoplasm. The 90° rotation is for the bottom view for both HRs.

at different salt concentrations are shown along with time-dependent absorbance changes at 580 nm. The half-life of the ground state recovery is 4.17 and 3.23 ms of *Hm*HR and *Hw*HR respectively, under 4 M NaCl (Figures 2e and 2f). When exposed to a buffer of low ionic strength with 5 mM NaCl and 333 mM Na$_2$SO$_4$, the recovery times are slightly different in both HRs (Supplementary Table S2 and Figure S3 at http://www.bioscirep.org/bsr/032/bsr0320501add.htm).

Chloride-binding affinity of *Hm*HR and *Hw*HR

The *H. walsbyi* cells were shown to tolerate 2 M MgCl$_2$, an unusual environment for any other currently known HRs. To investigate this observation, the chloride-dependent spectral shifts of *Hw*HR and *Hm*HR were measured (Figure 3). The chloride-dependent spectral shift indicates the binding affinity of chloride ions to HRs, which is analogous to the binding behaviour of a ligand to a receptor, and it can be described via the Hill
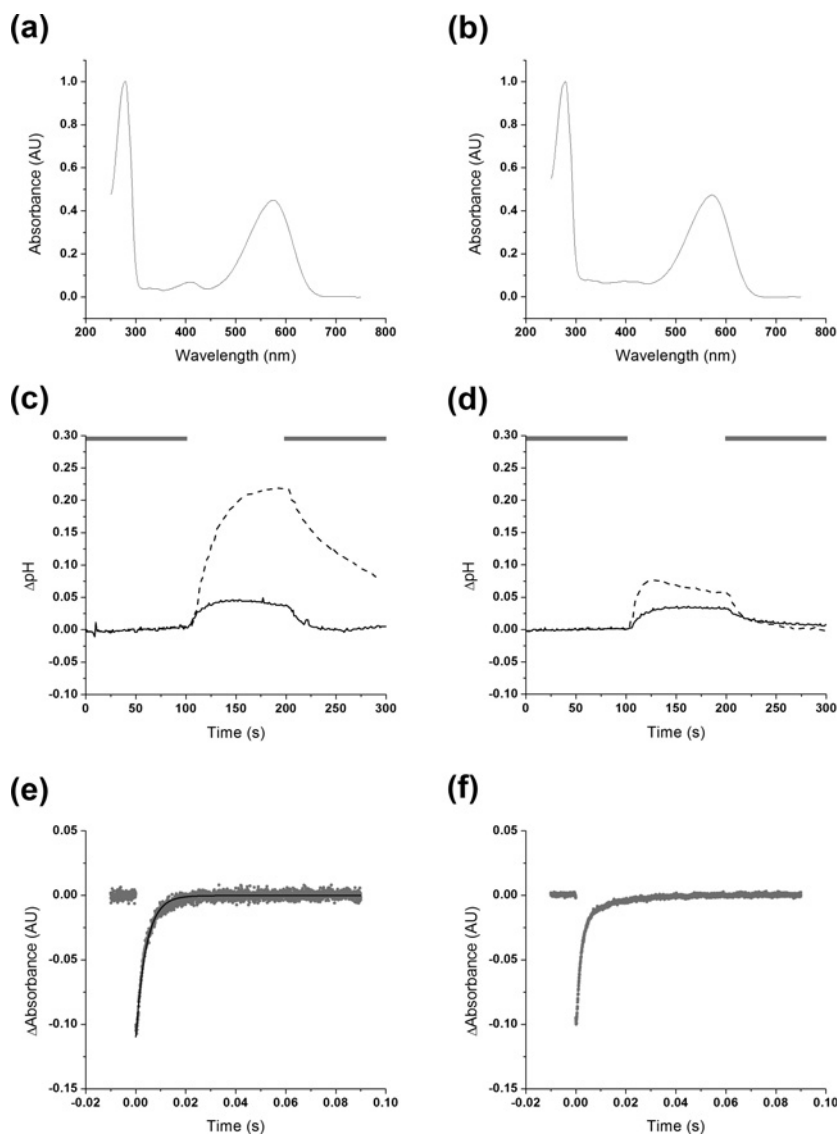
Figure 2   Spectroscopic characterization and functional determination of *Hm*HR and *Hw*HR
UV/Vis absorbance spectra of *Hm*HR (**a**) and *Hw*HR (**b**). The purified protein was resuspended in a buffer containing 50 mM Mes, 4 M NaCl, pH 5.8 and 0.05 % DDM. The passive proton uptake activity of *Hm*HR (**c**) and *Hw*HR (**d**) expressed in *E. coli* is shown. The grey bar region indicates the sample incubated under the dark condition, and the illumination period was 100 s, then followed by another 100 s of dark incubation. The solid line shows the sample treated without CCCP, and the dotted line indicates the sample with CCCP. Laser-induced absorbance changes of *Hm*HR (**e**) and *Hw*HR (**f**) under 50 mM Mes, 4 M NaCl and 0.05 % DDM, pH 5.8. The absorbance change was monitored at 580 nm. The data were analysed and fitted to one exponential decay (shown as a black line) for photocycle recovery half time.

equation [21]. The results showed that, for *Hm*HR (Figure 3a), an approximately 15 nm shift was observed in conditions of less than 1 M of chloride. The spectral shifts ceased at 591 nm when the concentration of NaCl fell below 1 mM, and the so-called 'blue HR' (Figure 3a, inset) was formed as observed in other studies [11,19]. *Hm*HR had no spectral changes from 4 to 1 M NaCl. *Hw*HR (Figure 3b), by contrast, showed no significant spectral shift throughout various chloride concentrations, with only a slight 2–3 nm of either redshifted or blueshifted changes observed in the range of 250 mM to 15 μM NaCl before finally settling at 576 nm, close to the ground state.

Furthermore, when both *Hm*HR and *Hw*HR were placed in a low-chloride or chloride-free buffer, *Hm*HR became 'blue HR' as mentioned above, while *Hw*HR remained purple without a significant λ_{max} change (Figure 3b, inset). As previous studies showed that under very low chloride conditions, the λ_{max} of *Hs*HR [30] was reported to be 568 nm (a blueshift of approximately 10 nm from 578 nm), and the λ_{max} was 599 nm, a redshift of approximately 20 nm, in *Np*HR [21], *Hw*HR thus showed an exceptionally high tolerance to any chloride concentration changes.

Further analysis of the calculated difference spectra of *Hm*HR (Figure 3c) and *Hw*HR (Figure 3d) indicated that the decrease of
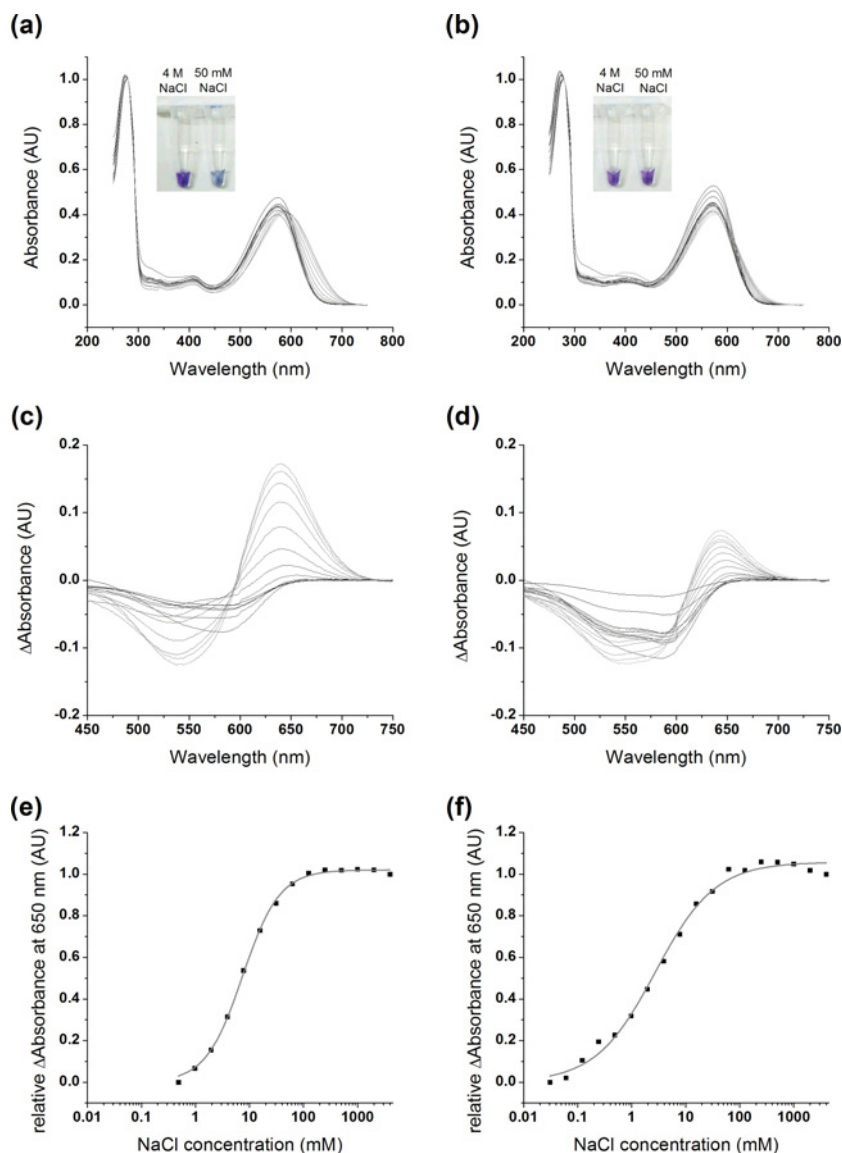
Figure 3   Chloride-dependent spectral changes in the absorption spectrum of HRs obtained from *E. coli* membrane
The spectral changes of *Hm*HR (**a**) and *Hw*HR (**b**); the corresponding difference spectra of *Hm*HR (**c**) and *Hw*HR (**d**); the absorbance change at 650 nm of *Hm*HR (**e**) and *Hw*HR (**f**) are shown, respectively. Purified HRs were incubated in the buffer solutions, which consisted of 50 mM Mes, pH 5.8, including 0.05 % DDM and the appropriate amount of NaCl. In (**a**, **b**), the insert pictures show the purified HR, which was resuspended under the noted condition. In (**a**–**d**), the grey scale indicates the decrease of chloride concentrations. In (**e**, **f**), the absorbance changes were normalized and the solid line denotes the best-fitted model.

chloride concentration made both HRs show a decreased fraction at approximately 550 nm and an increased fraction at approximately 650 nm. An isosbestic point was observed at approximately 600 nm in *Hw*HR but not in *Hm*HR, further suggesting that a one-step transition conformational change from the chloride-unbinding to binding state occurred in *Hw*HR but not in *Hm*HR. The amplitude changes (ΔA) at 650 nm were used to determine the dissociation constant K_{d} values, and they were 7.47 mM (Figure 3e) and 2.74 mM (Figure 3f) for *Hm*HR and *Hw*HR respectively. Those values were similar to the previously reported 10 mM for *Hs*HR and 1 or 3 mM for *Np*HR [16,20,31], indic-

ating the similarity in chloride binding affinity among all four HRs.

The structural-based sequence analysis of HRs for the unique chloride-independent spectra feature
Further investigating the retinal binding pocket at approximately 10 Å (where 1 Å = 0.1 nm), we identified two unique residues that were not conserved only in *Hw*HR (Figures 1b and 1c); one was Thr[186] and the other was Ser[262] of *Hw*HR. Both residues are typically alanine in other known HRs (Figure 1b, and Supplementary Figure S1). According to a structural model created
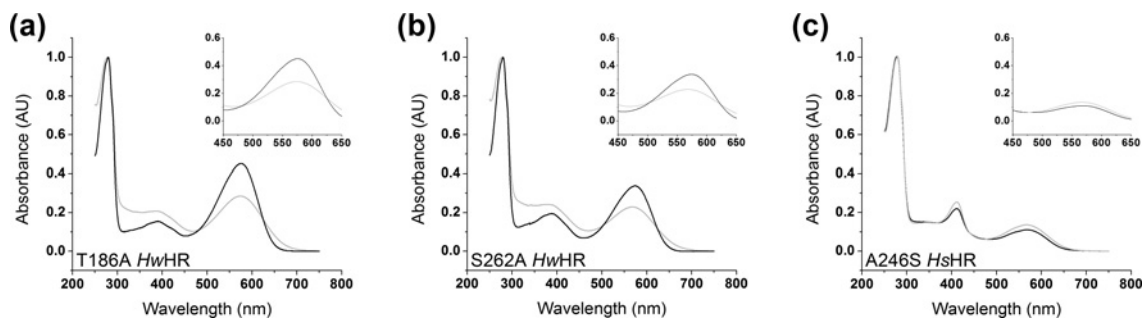
Figure 4   Chloride-dependent spectra of various mutants of *Hw*HR and A246S *Hs*HR
The UV/Vis spectra of T186A *Hw*HR (**a**), S262A *Hw*HR (**b**) and A246S *Hs*HR (**c**) were measured under different chloride concentrations to determine the chloride-dependent colour tuning. All purified proteins were dissolved in 50 mM Mes (pH 5.8) and 0.05% DDM buffer containing 4 M NaCl (black line) or 0 M NaCl (grey line).

with Swiss Model, the Thr[186] in *Hw*HR points out towards the membrane region on the helix E, but Ser[262] is orientated inward towards the Schiff base, the chloride-binding pocket on helix G (Figure 1c, right-hand panel).

The residue Ser[262] of *Hw*HR eliminated the unique feature of *Hw*HR in the chloride-dependent λ_{max} shift

As Thr[186] and Ser[262] are both typically conserved alanine residues in other known halobacterial HRs, single residue substitutions of T186A and S262A in *Hw*HR were constructed. The S262A-*Hw*HR eliminated the chloride-independent λ_{max} change feature (Figure 4b), as a blueshift of approximately 8 nm under low chloride conditions was observed but T186A-*Hw*HR (Figure 4a) behaved like the wild-type. However, the light-driven chloride-pumping capability and the photocycle of S262A were comparable with the wild-type (Supplementary Table S4 at http://www.bioscirep.org/bsr/032/bsr0320501add.htm). The chloride-binding affinity assay showed that the K_d was 10.40 mM for the S262A-*Hw*HR, comparable with *Hs*HR. The Hill coefficient (*n*) was 0.91, suggesting no significant change in chloride-binding from *Hw*HR.

*Hs*HR planted with corresponding Ser[262] showed no chloride-dependent λ_{max} change

The Ser[262] in *Hw*HR was engineered to *Hs*HR, which was determined to be closer in sequence alignment, in order to create an A246S-*Hs*HR, and the chloride-dependent λ_{max} shift was eliminated (Figure 4c, and Supplementary Table S4); it showed a stable λ_{max} at 568 nm from 4 M to 0.4 mM NaCl solutions.

DISCUSSION

HR proteins represent an effective biological mechanism that directly elevates the capability of early life forms to cope with extremely high salt environments, which is the case for most *Halobacteria*. In the present study, *Hw*HR from *H. walsbyi* was

shown to function as a light-driven chloride transporter with a stable λ_{max} even under almost chloride-free conditions, a feature not yet observed in any other known HRs. The serine residue at position 262 of *Hw*HR was found to act as a spectrum stabilizer, causing such chloride-independent λ_{max} change.

Chloride binding is known to be important for maintaining a stable λ_{max}, but the chloride-binding network in *Hw*HR might have slight variations from other known HRs. According to the structural model of *Hw*HR (Figure 1c), the Ser[262] located at helix G faces the Thr[66] at helix B, and together they can form a chloride stabilizer with their polar hydroxyl groups. Thr[66] is known to be important in chloride translocation paths, and Ser[262] is an alanine, a non-polar group, in all other annotated HRs except for *Natrialba magadii* and *Salinibacter ruber*. When A246S-*Hs*HR was constructed to have this Ser[262] corresponding to *Hw*HR, the chloride-dependent λ_{max} shift was eliminated, and it stayed at 568 nm from 4 M to 0.4 mM NaCl solutions.

It is mainly retinal and its surrounding chemical environment that contribute the colour, or absorbance, of a retinal-binding protein. Retinal divides the HRs into extracellular and cytoplasmic regions. Among them, residues Arg[108]/Thr[111] locate in the extracellular region in *Hs*HR and they are involved in transportation of an anion into the cytoplasmic region, which contains three conserved residues, Thr[66]/Arg[200]/Thr[203] [32,33]. On the other hand, the Ser[262] in *Hw*HR and Ala[246] in *Hs*HR identified in the present study appear to locate near the cytosolic region containing conserved residues Thr[82]/Arg[216]/Thr[219] in *Hw*HR and Thr[66]/Arg[200]/Thr[203] in *Hs*HR that were known to be important for chloride translocation. Specifically, during the catalytic cycle of HRs, the chloride ion was proposed to move to Thr[203] before being released into the cytosol [18,34]. Therefore a slightly different chloride translocation network in the cytoplasmic region formed via residues Thr[82]/Arg[216]/Thr[219]/Ser[262] in *Hw*HR can be thus proposed.

This explanation is consistent with previously reported observations that the λ_{max} shifts occur in various HRs (Supplementary Figure S4) under 0–4 M NaCl environments: *Np*HR [20] showed a 22 nm blueshift, a 13 nm redshift in *Hs*HR [19] and a 15 nm blueshift in *Hm*HR, while either a red- or blueshift within 3 nm was detected in *Hw*HR. In the chloride-free

environment, *Hw*HR was the only HR that showed no conversion into the so-called 'purple HR' Other results in the present study also support *Hw*HR having a different chloride binding conformation. First, the lack of a clear isosbestic point in *Hm*HR (Figure 4a) suggested that there are either multiple binding sites for the chloride or multiple conformations of the protein, but not in *Hw*HR. Secondly, the Hill coefficient depicts the co-operation of ligand binding, and *Hm*HR had a slightly larger Hill coefficient than that of *Hw*HR (n*Hm*HR = 1.27, n*Hw*HR = 0.79), suggesting that there was most likely a slight variation in the ionic network for chloride binding among the residues between *Hm*HR and *Hw*HR.

*Hw*HR might have a single chloride-binding site instead of two. Two chloride-binding sites were found in *Hs*HR [35], and they occurred in the Schiff-base region, as in most HRs, with a three-residue binding motif composed of two positively charged arginine residues and a glutamate residue. Sequence analysis (Figure 1b, and Supplementary Figure S1) showed the second non-Schiff base chloride-binding site, which stabilized chloride with residues Arg^{24}, Arg^{103} and Gln^{105} in *Hs*HR, is not conserved in *Hw*HR.

As the hydroxy groups exist in both side chains of serine and threonine, and both amino acids also occupy similar spaces in the side chains, the explanation for Ser^{262} to have such an impact in chloride-dependent λ_{max} changes of *Hw*HR requires further study.

In conclusion, *Hw*HR had an unexpectedly stable λ_{max} regardless of environmental chloride concentration, a feature not previously observed in any other HR. This feature is, at least partially, contributed by the residue Ser^{262}, and the residue's arrangement that is determined by the structural conformation can explain this observation. This unique tolerance of *Hw*HR for a chloride-free environment could further provide information in understanding the colour tuning in HR and the strategies adopted by early life forms to survive ever-changing environments.

REFERENCES

1   Briggs, W. R. and Spudich, J. L. (2006) Handbook of photosensory receptors, Wiley–VCH, New York

2   Oesterhelt, D. and Stoeckenius, W. (1971) Rhodopsin-like protein from the purple membrane of *Halobacterium halobium*. Nat. New. Biol. **233**, 149–152

3   Matsuno-Yagi, A. and Mukohata, Y. (1980) ATP synthesis linked to light-dependent proton uptake in a rad mutant strain of *Halobacterium* lacking bacteriorhodopsin. Arch. Biochem. Biophys. **199**, 297–303

4   Schobert, B. and Lanyi, J. K. (1982) Halorhodopsin is a light-driven chloride pump. J. Biol. Chem. **257**, 10306–10313

5   Bogomolni, R. A. and Spudich, J. L. (1982) Identification of a third rhodopsin-like pigment in phototactic *Halobacterium halobium*. Proc. Natl. Acad. Sci. U.S.A. **79**, 6250–6254

6   Spudich, J. L. and Bogomolni, R. A. (1984) Mechanism of colour discrimination by a bacterial sensory rhodopsin. Nature **312**, 509–513

7   Takahashi, T., Mochizuki, Y., Kamo, N. and Kobatake, Y. (1985) Evidence that the long-lifetime photointermediate of s-rhodopsin is a receptor for negative phototaxis in *Halobacterium halobium*. Biochem. Biophys. Res. Commun. **127**, 99–105

8   Falb, M., Pfeiffer, F., Palm, P., Rodewald, K., Hickmann, V., Tittor, J. and Oesterhelt, D. (2005) Living with two extremes: conclusions from the genome sequence of *Natronomonas pharaonis*. Genome Res. **15**, 1336–1343

9   Bolhuis, H., Palm, P., Wende, A., Falb, M., Rampp, M., Rodriguez-Valera, F., Pfeiffer, F. and Oesterhelt, D. (2006) The genome of the square archaeon *Haloquadratum walsbyi*: life at the limits of water activity. BMC Genomics **7**, 169

10 Sudo, Y., Ihara, K., Kobayashi, S., Suzuki, D., Irieda, H., Kikukawa, T., Kandori, H. and Homma, M. (2011) A microbial rhodopsin with a unique retinal composition shows both sensory rhodopsin II and bacteriorhodopsin-like properties. J. Biol. Chem. **286**, 5967–5976

11 Baliga, N. S., Bonneau, R., Facciotti, M. T., Pan, M., Glusman, G., Deutsch, E. W., Shannon, P., Chiu, Y., Weng, R. S., Gan, R. R. et al. (2004) Genome sequence of *Haloarcula marismortui*: a halophilic archaeon from the Dead Sea. Genome Res. **14**, 2221–2234

12 Fu, H. Y., Lin, Y. C., Chang, Y. N., Tseng, H., Huang, C. C., Liu, K. C., Huang, C. S., Su, C. W., Weng, R. R., Lee, Y. Y. et al. (2010) A novel six-rhodopsin system in a single archaeon. J. Bacteriol. **192**, 5866–5873

13 Wagner, G., Traulich, B., Hartmann, K. M. and Oesterhelt, D. (1987) Photochromic synergism of bacteriorhodopsin- and halorhodopsin-mediated photophosphorylation in *Halobacterium halobium*. Photochem. Photobiol. **46**, 393–402

14 Matsuno-Yagi, A. and Mukohata, Y. (1977) Two possible roles of bacteriorhodopsin; a comparative study of strains of *Halobacterium halobium* differing in pigmentation. Biochem. Biophys. Res. Commun. **78**, 237–243

15 Mukohata, Y. and Kaji, Y. (1981) Light-induced membrane-potential increase, ATP synthesis, and proton uptake in *Halobacterium halobium*, R1mR catalyzed by halorhodopsin: effects of N,N′-dicyclohexylcarbodiimide, triphenyltin chloride, and 3,5-di-tert-butyl-4-hydroxybenzylidenemalononitrile (SF6847). Arch. Biochem. Biophys. **206**, 72–76

16 Bivin, D. B. and Stoeckenius, W. (1986) Photoactive retinal pigments in haloalkaliphilic bacteria. J. Gen. Microbiol. **132**, 2167–2177

17 Seki, A., Miyauchi, S., Hayashi, S., Kikukawa, T., Kubo, M., Demura, M., Ganapathy, V. and Kamo, N. (2007) Heterologous expression of *Pharaonis* halorhodopsin in *Xenopus laevis* oocytes and electrophysiological characterization of its light-driven Cl-pump activity. Biophys. J. **92**, 2559–2569

18 Kolbe, M., Besir, H., Essen, L. O. and Oesterhelt, D. (2000) Structure of the light-driven chloride pump halorhodopsin at 1.8 Å resolution. Science **288**, 1390–1396

19 Kouyama, T., Kanada, S., Takeguchi, Y., Narusawa, A., Murakami, M. and Ihara, K. (2010) Crystal structure of the light-driven chloride pump halorhodopsin from *Natronomonas pharaonis*. J. Mol. Biol. **396**, 564–579

20 Schobert, B., Lanyi, J. K. and Oesterhelt, D. (1986) Effects of anion binding on the deprotonation reactions of halorhodopsin. J. Biol. Chem. **261**, 2690–2696

21 Sato, M., Kanamori, T., Kamo, N., Demura, M. and Nitta, K. (2002) Stopped-flow analysis on anion binding to blue-form halorhodopsin from *Natronobacterium pharaonis*: comparison with the anion-uptake process during the photocycle. Biochemistry **41**, 2452–2458

22 Scharf, B. and Engelhard, M. (1994) Blue halorhodopsin from *Natronobacterium pharaonis*: wavelength regulation by anions. Biochemistry **33**, 6387–6393

23 Chizhov, I. and Engelhard, M. (2001) Temperature and halide dependence of the photocycle of halorhodopsin from *Natronobacterium pharaonis*. Biophys. J. **81**, 1600–1612

24 Gradinaru, V., Thompson, K. R. and Deisseroth, K. (2008) eNpHR: a *Natronomonas* halorhodopsin enhanced for optogenetic applications. Brain Cell Biol. **36**, 129–139

25 Anton, J., Llobet-Brossa, E., Rodriguez-Valera, F. and Amann, R. (1999) Fluorescence *in situ* hybridization analysis of the prokaryotic community inhabiting crystallizer ponds. Environ. Microbiol. **1**, 517–523

26 Ng, W. V., Kennedy, S. P, Mahairas, G. G., Berquist, B., Pan, M., Shukla, H. D., Lasky, S. R., Baliga, N. S., Thorsson, V. and Sbrogna, J. (2000) Genome sequence of *Halobacterium* species NRC-1. Proc. Natl. Acad. Sci. U.S.A. **97**, 12176–12181

27 Sasaki, J., Brown, L. S., Chon, Y. S., Kandori, H., Maeda, A., Needleman, R. and Lanyi, J. K. (1995) Conversion of bacteriorhodopsin into a chloride ion pump. Science **269**, 73–75

28 Wang, W. W., Sineshchekov, O. A., Spudich, E. N. and Spudich, J. L. (2003) Spectroscopic and photochemical characterization of a deep ocean proteorhodopsin. J. Biol. Chem. **278**, 33985–33991

29 Sharma, A. K., Walsh, D. A., Bapteste, E., Rodriguez-Valera, F., Ford Doolittle, W. and Papke, R. T. (2007) Evolution of rhodopsin ion pumps in haloarchaea. BMC Evol. Biol. **7**, 79

30 Ogurusu, T., Maeda, A., Sasaki, N. and Yoshizawa, T. (1981) Light-induced reaction of halorhodopsin prepared under low salt conditions. J. Biochem. **90**, 1267–1273

31 Duschl, A., Lanyi, J. K. and Zimanyi, L. (1990) Properties and photochemistry of a halorhodopsin from the haloalkalophile, *Natronobacterium pharaonis*. J. Biol. Chem. **265**, 1261–1267

32 Rüdiger, M., Haupts, U., Gerwert, K. and Oesterhelt, D. (1995) Chemical reconstitution of a chloride pump inactivated by a single point mutation. EMBO J. **14**, 1599

33 Rüdiger, M. and Oesterhelt, D. (1997) Specific arginine and threonine residues control anion binding and transport in the light-driven chloride pump halorhodopsin. EMBO J. **16**, 3813–3821

34 Haupts, U., Tittor, J., Bamberg, E. and Oesterhelt, D. (1997) General concept for ion translocation by halobacterial retinal proteins: the isomerization/switch/transfer (IST) model. Biochemistry **36**, 2–7

35 Yamashita, Y., Kikukawa, T., Tsukamoto, T., Kamiya, M., Aizawa, T., Kawano, K., Miyauchi, S., Kamo, N. and Demura, M. (2011) Expression of *salinarum* halorhodopsin in *Escherichia coli* cells: solubilization in the presence of retinal yields the natural state. Biochim. Biophys. Acta **1808**, 2905–2912

Original Paper

SUPPLEMENTARY ONLINE DATA

Ser^{262} determines the chloride-dependent colour tuning of a new halorhodopsin from *Haloquadratum walsbyix*

Hsu-Yuan FU*[1], Yung-Ning CHANG*[1], Ming-Jin JHENG* and Chii-Shen YANG*†[2]

*Department of Biochemical Science and Technology, College of Life Science, National Taiwan University, 1 Roosevelt Road, Taipei 10617, Taiwan, and †Institute of Biotechnology, College of Bio-Resources and Agriculture, National Taiwan University, 1 Roosevelt Road, Taipei 10617, Taiwan

See the following pages for Supplementary Figures S1–S4 and Supplementary Tables S1–S4.

[1] These authors contributed equally to this work.
[2] To whom correspondence should be addressed (email chiishen@ntu.edu.tw).
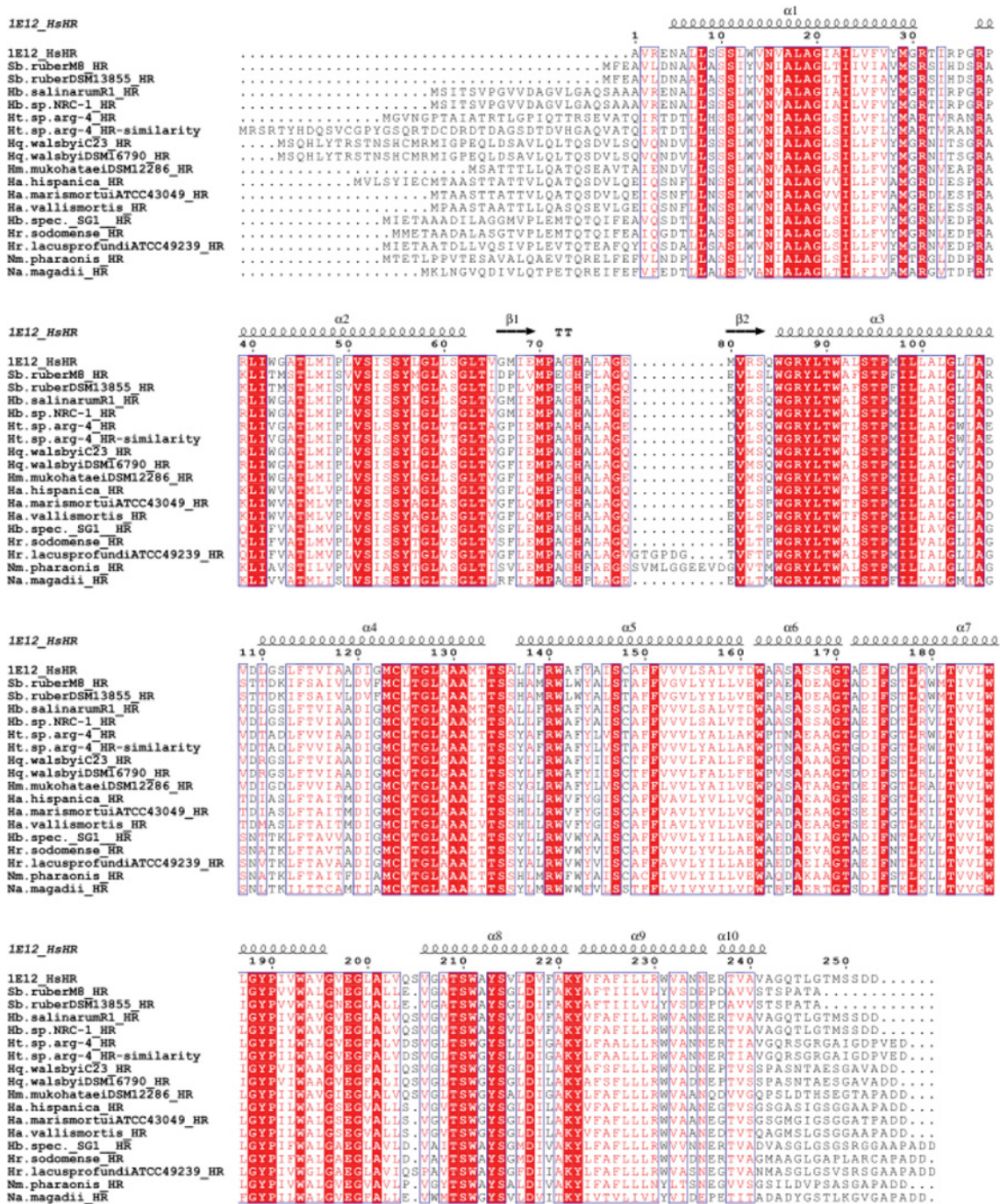
Figure S1   Sequence alignments with secondary structure information of all known HRs

Amino acids are marked with a red background or red colour representing high to low similarity, respectively. The atomic resolution structure information of *Hs*HR (PDB ID: 1E12) was used for secondary structure information, which is shown in the first row. The results were created by ESPript 2.2 [1].
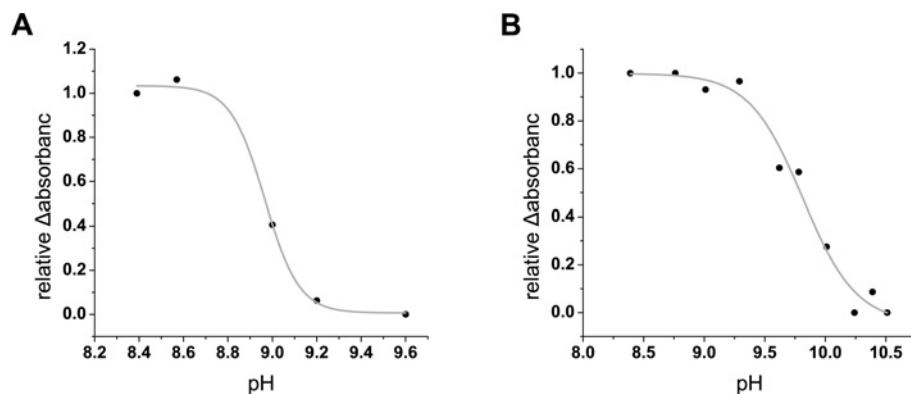
Figure S2 **Plots and fitting results of the pK_a determination of both *Hm*HR (A) and *Hw*HR (B)**
To study the spectral changes in acid or alkaline environments, a high concentration of HR sample in pH 5.8 (50 mM Mes and 4 M NaCl, pH 5.8) was diluted into different buffers with a pH of 3.095 to 10.93. In acidic conditions, both *Hm*HR and *Hw*HR showed a spectral shift of 7–9 nm toward the blue light region from the A_{max} of the ground state, whereas there were no significant spectral shifts in an alkaline environment; only the decrease in the ground state absorbance with a concomitant increase in the A_{410} species was observed. Spectral shifts from pH 8.4 to 10.5 were used to determine the pK_a of the Schiff base (Abs = $Abs_{acidic} + Abs_{basic-acidic}(10^{pH - pKa})$), and the calculated p$K_a$ values of *Hm*HR (**A**) and *Hw*HR (**B**) were 8.96 and 9.81 respectively.
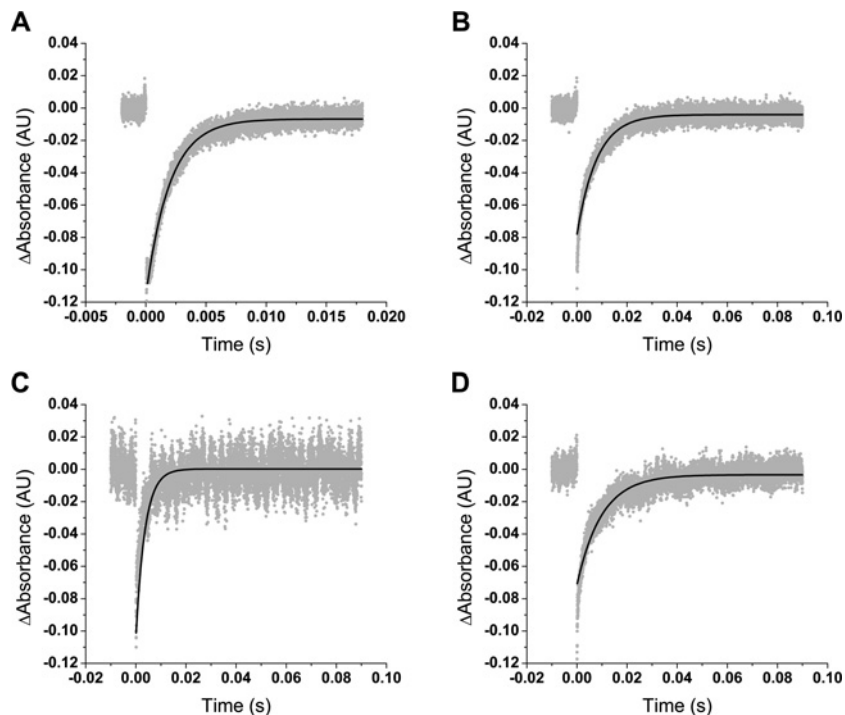
Figure S3   Laser-induced absorbance changes of HRs under different buffer conditions
The absorbance change was monitored at 570 nm. Both purified *Hm*HR and *Hw*HR suspended in the different buffer conditions mimic different physiological conditions. The results of *Hm*HR (**A**) and *Hw*HR (**B**) in 50 mM Mes, 5 mM NaCl, 333 mM Na_2SO_4 and 0.05% DDM, pH 5.8; and *Hm*HR (**C**) and *Hw*HR (**D**) in 50 mM Mops, 4 M NaCl and 0.05% DDM, pH 7.0, were analysed and fit to one exponential decay for photocycle recovery half time and are summarized in Supplementary Table S2.
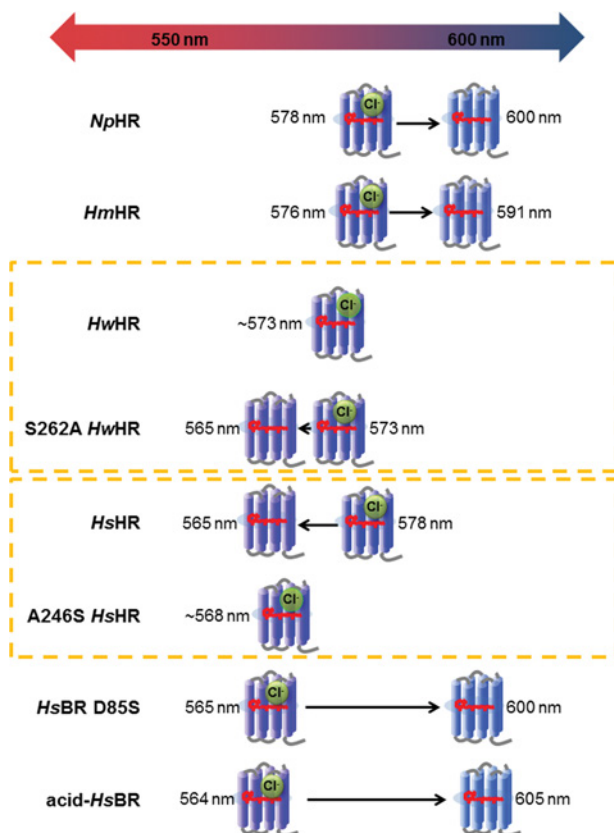
Figure S4 Summary of the maximum absorbance shift under chloride binding/non-binding forms in the previous study [2] and in the present study
The well-studied *Np*HR and *Hs*HR proteins have a 22 nm and 13 nm spectral shift respectively. *Hm*HR showed a similar absorbance change (15 nm) and trend (blueshift upon chloride binding) to those of *Hs*HR. The similar chemical environment of both the protonated Schiff base and the chloride transfer pathway were considered based on the action spectra in *Np*HR, *Hs*BR D85S, acid-*Hs*BR and *Hm*HR. *Hw*HR showed the most stable action spectrum under the different chloride conditions.

Table S1 Summary of known HRs in recent studies

Genemo project anotation is used. At least ten HRs appear in the NCBI database (as of 19 June 2012). −, not annotated; c, complement.

Organism	Gene name	Locus	Amino acid number	GenBank® accession no.
Prokaryota (Euryarchaeota)				
Halalkalicoccus jeotgali B3	−	−	−	−
Haloarcula hispanica	*hop*	c(2125932–2126786)	284	AEM57789.1
Haloarcula marismortui ATCC 43049	*hop*	c(1489351–1490181)	276	YP_136278.1
Halobacterium salinarum R1	*hop*	c(155843–156667)	274	CAP13054.1
Halobacterium sp. NRC-1	*hop*	c(155681–156505)	274	AAG18795.1
Haloferax mediterranei ATCC 33500	−	−	−	−
Haloferax volcanii DS2	−	−	−	−
Halogeometricum borinquense DSM 11551	−	−	−	−
Halomicrobium mukohataei DSM 12286	−	1007876–1008697	273	ACV47184.1
Haloquadratum walsbyi DSM 16790	*hop*	c(2371913–2372791)	292	CAJ53165.1
Halorhabdus utahensis DSM 12940	−	−	−	−
Halorubrum lacusprofundi ATCC 49239	−	c(590870–591745)	291	ACM56176.1
Haloterrigena turkmenica DSM 5511	−	−	−	−
Natronomonas pharaonis DSM 2160	*hop*	c(327687–328562)	291	CAI48412.1
Natrialba magadii ATCC 43099	−	2653987–2654826	279	ADD06141.1
Halopiger xanaduensis SH-6	−	−	−	−
Haloquadratum walsbyi C23	*hop*	c(2566001–2566879)	292	CCC41335.1
Prokaryota (bacteroidetes/chlorobi)				
Salinibacter ruber DSM 13855	−	3439239–3439988	249	ABC44173.1
Salinibacter ruber M8	*Halorhodopsin*	3510167–3510916	249	CBH25915.1
Protein sequenced				
Halobacteriaceae gen. sp.	*Halorhodopsin*	A56808	239 (fragment)	−
Haloterrigena sp. *arg-4*	*Halorhodopsin*	BAA75201	282	BAA75201.2
Halorubrum sodomense	*Halorhodopsin*	BAA75202	282	BAA75202.1
Halobacterium sp. SG1	*Halorhodopsin*	CAA49773	284	CAA49773.1
'*Haloterrigena*' sp. (strain arg-4)	*Halorhodopsin*	T43838	297	−
Haloarcula vallismortis	*Cruxhalorhodopsin*-3	BAA06679	276	BAA06679.1

Table S2 Summary of the the half-time of the ground state recovery of *Hm*HR and *Hw*HR in various conditions

Protein	50 mM Mes, 4 M NaCl and 0.05 % DDM, pH 5.8	50 mM Mes, 5 mM NaCl, 333 mM Na$_2$SO$_4$ and 0.05 % DDM, pH 5.8	50 mM Mops, 4 M NaCl and 0.05 % DDM, pH 7.0
*Hm*HR	4.17 ms	2.02 ms	3.58 ms
*Hw*HR	3.23 ms	7.93 ms	9.87 ms

Table S3 Summary of the features of known HRs in the present and previous studies

The identities of these sequences of HRs, maximum absorbance values, pK_a values (Supplementary Figure S2) and disassociation constants of chloride anions (K_d) are compiled. The smallest spectral shift was observed in *Hw*HR.

Parameter	*Hs*HR*	*Np*HR†	*Hm*HR	*Hw*HR
Identity‡	—	55%	62%	68%
	55%	—	61%	56%
Maximum absorbance (nm)	578	575	576	573
pK_a	8.9 or 9.5	9.6	8.9	9.8
K_d (chloride)	10 mM (blueshift 10 nm)	3 mM (redshift 20 nm)	9.7 mM (redshift 15 nm)	4 mM (blueshift 3 nm)

*Data obtained from [3].
†Data obtained from [4].
‡Calculated from ClustalW (http://www.genome.jp/tools/clustalw/)

Table S4 Summarized spectral features and functions of the HRs in the present study

The maximum absorbance values, chloride-dependent spectral property, disassociation constants of chloride anions (K_d) photocycle and functions are compiled. — , not detectable.

Parameter	*Hm*HR	*Hw*HR	S262A *Hw*HR	A246S *Hs*HR
λ_{max}	576 nm	573 nm	573 nm	568 nm
Chloride-dependent absorbance change	15 nm (redshift)	3 nm (blueshift)	8 nm (blueshift)	0 nm
K_d (chloride)	7.47 mM	2.74 mM	10.88 mM	23.22 mM
Half-time of ground state recovery	4.17 ms	3.23 ms	3.28 ms	16.00 ms
Light-driven chloride translocation	Yes	Yes	Yes	—

REFERENCES

1 Gouet, P., Courcelle, E., Stuart, D. I. and Métoz, F. (1999) ESPript: analysis of multiple sequence alignments in PostScript. Bioinformatics **15**, 305–308

2 Kubo, M., Kikukawa, T., Miyauchi, S., Seki, A., Kamiya, M., Aizawa, T., Kawano, K., Kamo, N. and Demura, M. (2009) Role of Arg123 in light-driven anion pump mechanisms of *pharaonis* halorhodopsin. Photochem. Photobiol. **85**, 547–555

3 Schobert, B., Lanyi, J. K. and Oesterhelt, D. (1986) Effects of anion binding on the deprotonation reactions of halorhodopsin. J. Biol. Chem. **261**, 2690–2696

4 Scharf, B. and Engelhard, M. (1994) Blue halorhodopsin from *Natronobacterium pharaonis*: wavelength regulation by anions. Biochemistry **33**, 6387–6393